Communications: SIF Congress 2011

Hydration properties of carbohydrates:
A clue from molecular dynamics

L. Lupi

Dipartimento di Fisica, Università di Perugia - Via Pascoli, I-06123 Perugia, Italy

Summary. — A molecular dynamics (MD) simulation study is presented for the dynamics of the polarizability anisotropy of pure water and of water-trehalose solutions as a function of concentration. The calculated time correlation functions (TCF) of the water collective polarizability for the different mixtures are compared and analyzed in terms of two distinct relaxation dynamics in the picoseconds timescale. The two processes have been attributed to the dynamics of bulk and hydration water molecules, respectively, with a retardation factor ~ 5. The whole picture has been confirmed by the further separation of the total water TCFs into the ones arising from bulk, hydration molecules and a cross term between the two, that allowed a separate estimate of the two relaxation times.

PACS `33.20.Fb` – Raman and Rayleigh spectra (including optical scattering).
PACS `33.20.Kf` – Visible spectra.

1. – Introduction

Water is known to play an important role in many biological processes such as protein-enzyme interactions, molecular recognition, and folding-unfolding phenomena [1, 2]. Moreover, most of the known proteins carry out their biological activity in water, and result to be inactive in the absence of the aqueous solvent. In particular, hydrophobic and hydrophilic interactions are known to be of great importance for the stability and the functionality of the macromolecules, so that the aqueous solvent is thought to play an active part in the dynamics of the biomolecules itself. For this reason, the dynamics of the water molecules solvating biological systems, especially those at the interface, has been the object of intensive investigation during the past 30 years [3]. The experimental characterization of the hydration water dynamics is very challenging especially when one is dealing with a complex solute itself, like a protein can be; for this reason aqueous solutions of simpler molecules are often used. Among those, carbohydrates are particularly suitable, for being quite totally hydrophilic compound and also for being very interesting in itself. In fact, sugars are well known to possess a very strong conservative

capability strictly connected to the interrelation between carbohydrates and the aqueous solvent [4-6]. Despite the huge amount of theoretical and experimental investigations addressed to this topic in the last 20 years [7-12], the interest on the dynamical and structural properties of aqueous solutions of carbohydrates is even grown.

Computational and experimental studies agree in reporting that hydration water molecules around carbohydrates show strong differences in their dynamics with respect to the bulk ones. Nevertheless, while general consensus is found on the existence of slowing-down of both translational and rotational mobility of water molecules in the vicinity of a carbohydrate [13-22], the extension and the entity of the retardation is still strongly debated. In fact, to experimentally probe the hydration dynamics is very challenging because it requires the selectivity to distinguish hydration from bulk-like dynamics in addition to the ability of separating the solvent dynamics from that of the solute. Recently, extended depolarized light scattering experiments [23-26] resulted to be a suitable tool to disentangle these different dynamics and to give an independent estimate of both the number of perturbed water molecules and the entity of the slowing-down. In the present work, with the use of molecular dynamics simulation, the challenge of how much water molecules are retarded by a single trehalose molecule is addressed. In particular the polarizability anisotropy relaxation of water in the presence of trehalose has been calculated from MD trajectories, and analyzed in terms of two distinct relaxation processes. The same quantity has been evaluated separately for the water molecules within the first hydration shell of the solute and for those far from the carbohydrate surface, confirming the general picture of the two distinct water species hypothesized for the interpretation of the total water TCFs.

2. – Theoretical background

The collective polarizability tensor, $\overline{\overline{\Pi}}$, for a condensed-phase system composed by N molecules can be expressed as a sum of molecular $\overline{\overline{\Pi}}^M$ and induced $\overline{\overline{\Pi}}^I$ contributions,

$$(1) \qquad\qquad \overline{\overline{\Pi}} = \overline{\overline{\Pi}}^M + \overline{\overline{\Pi}}^I,$$

where the molecular part is simply given by the sum of the intrinsic molecular polarizabilities $\overline{\alpha}_i^0$,

$$(2) \qquad\qquad \overline{\overline{\Pi}}^M = \sum_{i=1}^{N} \overline{\alpha}_i^0.$$

The induced contribution, $\overline{\overline{\Pi}}^I$, arises from interactions between molecular induced dipoles, it depends on orientational, conformational and translational degree of freedom and it can be interpreted as a dynamical modulation of the polarizabilities. In this work, this modulation arises from center-center dipolar coupling between the molecules, expressed by the dipole-induced-dipole model (DID)

$$(3) \qquad\qquad \overline{\overline{\Pi}}^I = \sum_{i=1}^{N} \overline{\alpha}_i^0 \cdot \overline{T}_{ij} \cdot \overline{\alpha}_j,$$

where $\overline{\alpha}_i^0$ are the molecular-induced polarizabilities and $\overline{T}_{ij} = \overline{T}(\overline{r}_{ij})$ is the dipole tensor between molecules i and j, and $\overline{r}_{ij}$ represents the vector connecting the two centers of mass. The dipole tensor is given by the usual expression

$$(4) \qquad \overline{T}(\overline{r}_{ij}) = \frac{3\hat{r}\hat{r} - \overline{1}}{r^3} \,.$$

In practice, being water molecules not highly polarizable, the less expensive first-order solution of eq. (3) has been employed.

The dynamics of interest are given by the time correlation function (TCF) of the off-diagonal elements of the collective polarizability tensor,

$$(5) \qquad \Psi(t) \cong \langle \Pi_{xz}(0)\Pi_{xz}(t) \rangle.$$

Moreover, based on eq. (1), $\Psi(t)$ can be separated into three terms, $\Psi^{MM}(t)$, $\Psi^{II}(t)$ and $\Psi^{MI}(t)$, arising from the autocorrelations of molecular and induced polarizabilities, and the cross term between the two.

3. – Results and discussion

The molecular dynamics simulation was carried out using the DL_POLY2.0 package [27]. The water intrinsic molecular polarizability tensor employed in the calculations were taken from *ab initio* quantum-chemical calculations at the MP3/6-31 + G$(2df, p)$ level [28]. The MD trajectories were generated using the SPC/E potential model for water [29], while intermolecular and intramolecular interactions for trehalose have been modeled with the use of the OPLS intermolecular potential function developed by Jorgensen *et al.* [30]. Intramolecular distances between atoms were kept fixed by using the SHAKE iterative procedure. The constraint method was used to integrate the equations of motion of the rigid molecules, in combination with the Verlet algorithm, with a time step of 5 fs. In addition to the pure water, aqueous mixtures for trehalose mole fractions of $X_{\mathrm{TRE}} = 0.004, 0.009, 0.02,$ and 0.04 have been studied. The simulations were performed in the microcanonical ensemble with a total number of $N = 200$–250 molecules placed in a cubic box with periodical boundary conditions, dimensioned to reproduce the experimental densities measured at room temperature. Short-ranged intermolecular interactions were cut off at half the box length, while standard Ewald sums with conducting boundaries were used to handle long-range Coulombic forces. Preliminary trajectories of 200 ps were first run for equilibration at 300 K; after this period the trajectories were saved and 2 ns runs were used to compute the quantities of interest. TCFs have been calculated up to tens of ps and are averaged over uncorrelated runs to get a higher statistics.

Figure 1 shows the polarizability anisotropy TCFs for water, $\Psi^W(t)/\Psi^W(0)$, normalized to their initial value, for pure water and for trehalose-water solutions at different compositions. The fast librational oscillations at short times are followed by a diffusive tail that results to be markedly affected by mixing. Both the two semi-log representations in the left and right panel of fig. 1 well show that the long time decay of the collective polarizability anisotropy correlations exhibits a substantial slowing-down as the trehalose mole fraction increases in the mixtures. In particular pronounced jumps are observed in the decay rate of $\Psi^W(t)$ as soon as a small amount of trehalose is added.
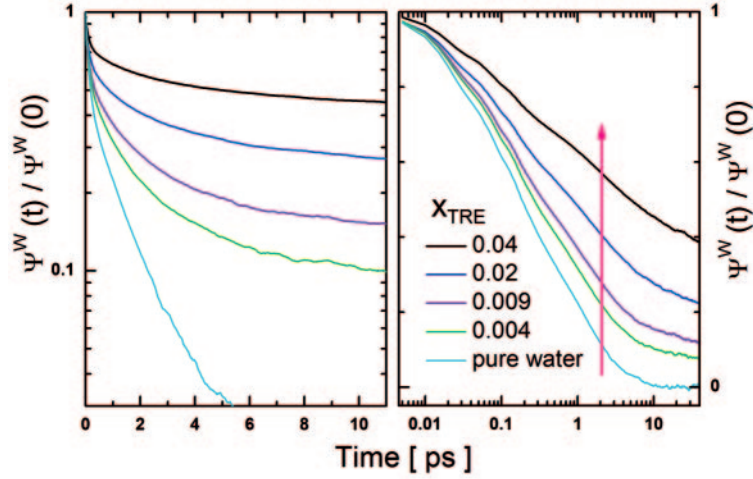
Fig. 1. – (Colour on-line) Water polarizability anisotropy relaxation in the case of pure water and of water-trehalose solutions at four different mole fractions at $300\,\mathrm{K}$, $\Psi^W(t)/\Psi^W(0)$. Left panel: log-scale in vertical axis. Right panel: log-scale in horizontal axis, fitting curve in red lines.

In order to identify the molecular origin of the different features that characterize the dynamics of water upon mixing, the TCFs of the collective polarizability anisotropy are analyzed in terms of the intrinsic and induced polarizability contributions, plus the cross-correlation between the two. Figure 2 shows the relaxation of the total anisotropy for water and its separate contributions, $\Psi^{W,MM}(t)$, $\Psi^{W,II}(t)$ and $\Psi^{W,MI}(t)$, in the case of bulk water (left panel) and water in a $X_{\mathrm{TRE}} = 0.02$ mole fraction solution (right panel).
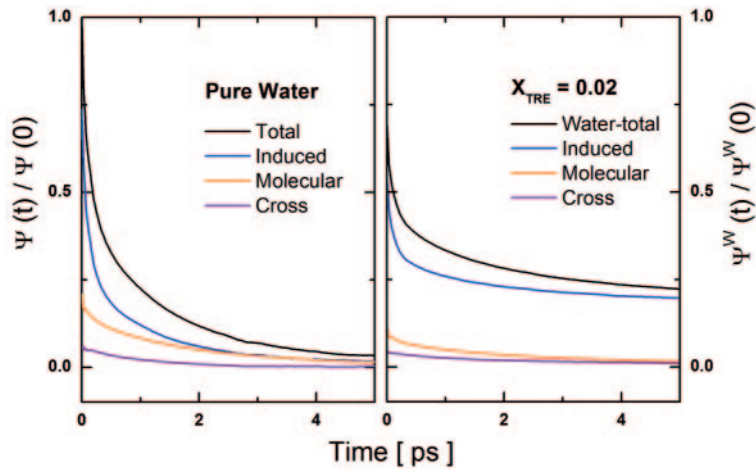

Fig. 2. – (Colour on-line) Water polarizability anisotropy relaxation $\Psi^W(t)/\Psi^W(0)$ (black line) and the corresponding contribution from molecular (orange line), induced (blue line), and molecular-induced cross terms (purple line), for pure water (left panel) and for $X_{\mathrm{TRE}} = 0.02$ (right panel) at $300\,\mathrm{K}$.
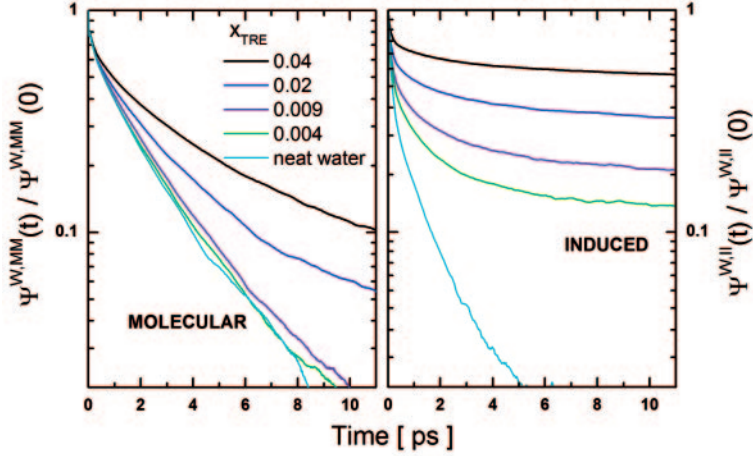
Fig. 3. – Water polarizability anisotropy relaxation for pure water and for water-trehalose solutions arising separately from molecular (left panel) and induced (right panel) contribution.

It can be seen (left panel) that the major contribution to the dynamics of water in the ps timescale comes from the induced component. This component, especially for not highly polarizable molecules like water, depends mainly on the intermolecular separation of the molecules, and is known to be strongly affected by the relaxation rate of the hydrogen bond network of the mixtures [31, 32]. Moreover the molecular component exhibits the fastest relaxation rate, while the induced one the slowest. Finally, the cross component results to be positive in the whole time scale displayed. As trehalose is added to water the decomposition of the TCFs of water into molecular, induced and cross-contribution shows (fig. 2, right panel) the same characteristic behavior of pure water, indicating that the molecular mechanism underlying water dynamics keeps being dominated by translational dynamics also upon mixing. Moreover, as for the tail at long times observable in water dynamics upon mixing, it can be noticed from fig. 3 that the induced contribution results to be the most perturbed one, while a small slowing-down is revealed for the molecular contribution as the trehalose mole fraction grows. From that it can be argued that the slowing-down imposed on water molecules by the presence of the sugar is mostly related to a translational dynamics. Despite the fact that the molecular contribution shows quite a slowing-down going from pure water up to the highest concentration of trehalose, it can be stated that the major contribution to the long times decay of water resides in the translational dynamics which is also the one which, as can be seen, constitutes the major contribution to the polarizability dynamics of water in its pure form and in solution. Going further on the investigation of water dynamics upon mixing, it can be observed that, while in the case of pure water, the TCF obtained from our simulation at 300 K has been fitted to a single Kohlrausch-Williams-Watts (KWW) function, with characteristic time and stretching parameter in good agreement with previous simulation results [32]; in the case of water in the presence of trehalose, the additional tail at long times, does not allow to fit the TCFs to a single KWW function. Computational and experimental results have found that hydration water, that is water in direct contact with biological molecules, shows strong differences in its dynamics with respect to the bulk. Following this idea and in analogy with well-established procedures [31,23,22], the water TCFs as a function of trehalose concentration are analyzed as the sum of two distinct contributions,
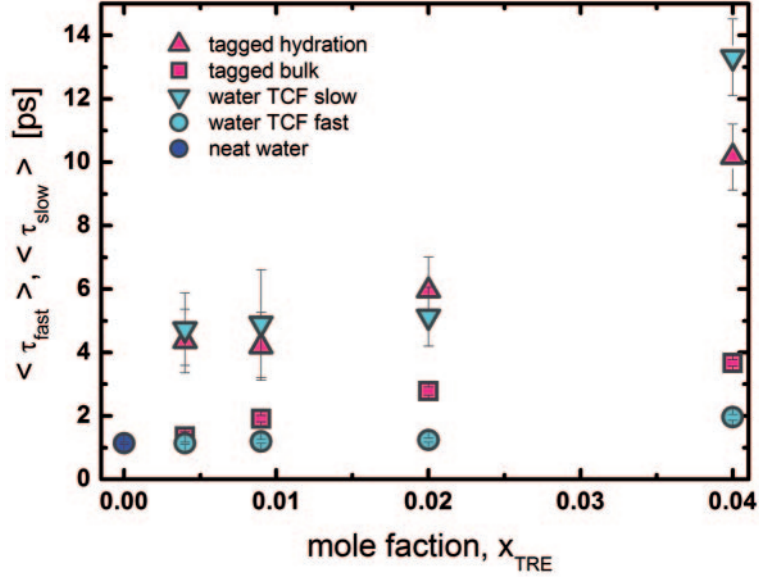
Fig. 4. – (Colour on-line) Relaxation time of bulk (blue squares) and hydration water (blue triangles) obtained from the fit of total water TCFs as a function of concentration, together with the relaxation times obtained by the fitting procedure of the partial bulk and hydration TCFs (pink diamond and pink triangle, respectively). The relaxation time obtained for pure water is also reported (cyan full circle).

taking into account the dynamic behavior of hydration and bulk water molecules. The 0.4–20 ps region has been reproduced by

$$(6) \qquad \Psi^W(t) = \Delta_{\text{bulk}} e^{-\left(\frac{t}{\tau_{\text{bulk}}}\right)^{\beta}} + \Delta_{\text{hydr}} e^{-\left(\frac{t}{\tau_{\text{hydr}}}\right)^{\beta}},$$

where Δ_{bulk} and Δ_{hydr} are the amplitudes and τ_{bulk} and τ_{hydr} the relaxation times of, respectively, bulk and hydration water molecules.

A first KWW function is used to model the contribution of bulk water with a characteristic relaxation time centered around 1 ps, very close to the value obtained for pure water. A second one has been used to reproduce the intensity in the $\sim$ 5–20 ps region, assigned to the dynamics of hydration water. The stretching parameter β has been fixed to the value obtained from the fitting of the calculated TCFs for pure water, $\beta = 0.6$, that is also in agreement with previous literature results [33-35,23], while the relaxation times and amplitudes are left free. We see in fig. 1 that this functional form is able to reproduce perfectly the shape of the TCFs of water molecules for all trehalose mole fractions. The concentration dependence of the average relaxation times of bulk and hydration water, obtained from the stretched exponential parameter by the relation $\langle \tau \rangle = \frac{\tau_{KWW}}{\beta} \Gamma(\frac{1}{\beta})$, is shown in fig. 4. The retardation ratio ξ between hydration and bulk water, almost concentration independent, is found to assume values around $\sim$ 5, in good agreement with previous depolarized light scattering findings [23].

As ca be seen, simulation methods are suitable for being selective in the molecule and molecular mechanism involved in a more complex process. Hence to further stress this ability, TCFs separately originating from hydration and bulk water molecules have
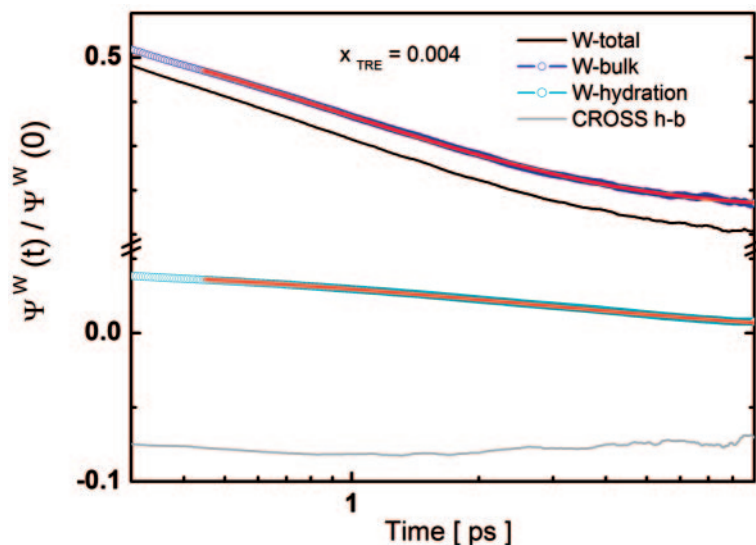
Fig. 5. – (Colour on-line) TCFs of the water collective polarizability anisotropy and its contribution from hydration, bulk water molecules and a cross term between the two for the $X_{\mathrm{TRE}} = 0.004$, fitting curve in red lines.

been calculated, and again, being the quantity of interest a collective one, the total water TCFs will have contributions arising from bulk, hydration and a cross-correlation between the two. In order to separare hydration from bulk water molecules, the water molecules in the simulation box have been tagged and divided into two classes according to the criterion in which a water molecule belongs to the first solvation shell of the solute if its oxygen atom is at a distance less than 3.1Å from each of the solute atoms, and the water TCFs separately originating from hydration and bulk water molecules have been calculated. Figure 5 shows the water TCF for a trehalose mole fraction of $X_{\mathrm{TRE}} = 0.004$, together with its separate contributions, $\Psi^{W,\mathrm{bulk}}(t)$, $\Psi^{W,\mathrm{hydr}}(t)$ and $\Psi^{W,\mathrm{bh}}(t)$. The TCFs obtained by this further separation have been fitted both to a single KWW function with stretching parameter $\beta = 0.6$ and with two distinct relaxation times, closely resembling the two obtained from the fitting procedure of the total water TCFs, with a faster time for the partial bulk contribution similar to that of pure water and a slower one for the partial hydration contribution. The results for this fitting procedures are shown in fig. 4 together with the results previously obtained from the fitting of the total water TCFs. It can be observed that the agreement between the two procedures is very good for the most dilute concentration, while it is not as much satisfying as the content of sugar in water increases. In this respect it can be observed that for the most dilute solutions the cross-correlation between bulk and hydration appears to be a slowly varying function of time and, thus, it makes a quite negligible contribution to the dynamics, while as soon as the trehalose concentration increases the cross term ends to be totally negligible, both in intensity and in contributing to the dynamics.

As a whole, the present analysis supports the hypothesis of considering the water dynamics in aqueous solutions of trehalose as composed of two well-distinct contributions, one arising from water molecules belonging to the hydration shell of the carbohydrate, in direct contact with its surface, and one from those outside the first hydration shell, also called *bulk-like* water molecules.

4. – Conclusions

Molecular dynamics simulations of the polarizability anisotropy relaxation have been carried out for water and water-trehalose solutions, showing that water slow dynamics in the presence of disaccharides exhibits two well-distinct relaxation processes, a faster one reasonably associated to water molecules far from the solute interface and a slower one characterizing hydration water molecules. This picture has been confirmed by the separate calculation of the polarizability correlation of water in and outside the first hydration shell that allowed to show that the two species of water molecules actually have two distinct characteristic relaxation times.

REFERENCES

[1] Janin J., *Structure*, **7** (1999) R277.
[2] Bagchi B., *Chem. Rev.*, **105** (2005) 3197.
[3] Tarek M. and Tobias D. J., *Phys. Rev. Lett.*, **88** (2002) 138101/1.
[4] Carpenter J. F. and Crowe J. H., *Biochemistry*, **28** (1989) 3916.
[5] Crowe J. H., Crowe L. M. and Chapman D., *Science*, **223** (1984) 701.
[6] Cesàro A., *Nat. Mater.*, **5** (2006) 593.
[7] Ding S. P., Fan J., Green J. L., Lu Q., Sanchez E. and Angell C. A., *J. Thermal Anal.*, **47** (1996) 1391.
[8] Sussich F., Urbani R., Princivalle F. and Cesàro A., *J. Am. Chem. Soc.*, **120** (1998) 7893.
[9] Branca C., Magazù S., Maisano G. and Migliardo P., *J. Chem. Phys.*, **111** (1999) 281.
[10] Branca C., Magazù S., Maisano G., Migliardo F., Migliardo P. and Romeo G., *J. Phys. Chem. B*, **105** (2001) 10140.
[11] Villarreal M. A., Diaz S. B., Disalvo E. A. and Montich G. G., *Langmuir*, **20** (2004) 7844.
[12] Lerbret A., Bordat P., Affouard F., Descamps M. and Migliardo F., *J. Phys. Chem. B*, **109** (2005) 11046.
[13] Sakurai M., Murata M., Inoue Y., Hino A. and Kobayashi S., *Bull. Chem. Soc. Jpn.*, **70** (1997) 847.
[14] Qiang Liu, Schmidt R. K., Teo B., Karplus P. A. and Brady J. W., *J. Am. Chem. Soc.*, **119** (1997) 7851.
[15] Bonanno G., Noto R. and Fornili S. L., *J. Chem. Soc., Faraday Trans.*, **94** (1998) 2755.
[16] Lee S. L., Debenedetti P. G. and Errington J. R., *J. Chem. Phys.*, **122** (2005) 204511.
[17] Choi Y., Cho K. W., Jeong K. and Jung S., *Carbohydrate Res.*, **341** (2006) 1020.
[18] Heyden M., Brundermann E., Heugen U., Niehues G., Leitner D. M. and Havenith M., *JACS*, **130** (2008) 5773.
[19] Sonoda M. and Skaf M. S., *J. Phys. Chem. B*, **111** (2007) 11948.
[20] Heugen U., Schwaab G., Brundermann E., Heyden M., Yu X., Leitner D. M. and Havenith M., *Proc. Natl. Acad. Sci. U.S.A.*, **103** (2006) 12301.
[21] Malsam J. and Aksan A. J., *Phys. Chem. B*, **113** (2009) 6792.
[22] Magno A. and Gallo P., *J. Phys. Chem. Lett.*, **2** (2011) 977.
[23] Paolantoni M., Comez L., Gallina M. E., Sassi P., Scarponi F., Fioretto D. and Morresi A., *J. Phys. Chem. B*, **113** (2009) 7874.
[24] Perticaroli S., Comez L., Paolantoni M., Sassi P., Lupi L., Fioretto D., Paciaroni A. and Morresi A., *J. Phys. Chem. B.*, **114** (2010) 8262.
[25] Rossi B., Comez L., Fioretto D., Lupi L., Caponi S. and Rossi F., *J. Raman Spectrosc.*, **42** (2011) 1479.

[26] PERTICAROLI S., COMEZ L., PAOLANTONI M., SASSI P., MORRESI A. and FIORETTO D., *J. Am. Chem. Soc.*, **133** (2010) 12063.

[27] SMITH W. B. and FORESTER T. R., *DL_POLY_2.0* (CCLRC, Daresbury Laboratory, Daresbury, UK) 1997.

[28] SKAF M. S. and VECHI S. M., *J. Chem. Phys.*, **119** (2003) 2181.

[29] BERENDSEN H. J. C., GRIGERA J. R. and STRAATSMA T. P., *J. Phys. Chem.*, **91** (1987) 6269.

[30] DAMM W., FRONTERA A., TIRADO-RIVES J. and JORGENSEN W. L., *J. Comput. Chem.*, **18** (1997) 1955.

[31] ELOLA M. D. and LADANYI B. M., *J. Chem. Phys.*, **126** (2007) 084504.

[32] SONODA M. T., VECHI S. M. and SKAF M. S., *Phys. Chem. Chem. Phys.*, **7** (2005) 1176.

[33] SOKOLOV A. P., HURST J. and QUITMANN D., *Phys. Rev. B*, **51** (1995) 12865.

[34] TORRE R., BARTOLINI P. and RHIGHINI R., *Nature (London)*, **428** (2004) 296.

[35] SKAF M. S. and SONODA M. T., *Phys. Rev. Lett.*, **94** (2005) 137802.